LIMNOLOGY
and
OCEANOGRAPHY: METHODS

ASLO

Limnol. Oceanogr.: Methods 23, 2025, 176–190

doi: 10.1002/lom3.10671

NEW METHODS

Inferring microalgae density and net ecosystem production on soft sediments using infrared imaging

Anthony R. Ives,[1]* **Emily L. Adler**,[1] **K. Riley Book**,[1] **Jamieson C. Botsch**,[1,2] **Árni Einarsson**,[3] **Ian S. Hart**,[1] **Colin H. Ives**,[4] **Ian Jin**,[1,5] **Amanda R. McCormick**,[1] **Joseph S. Phillips**[6]

[1]Department of Integrative Biology, University of Wisconsin-Madison, Madison, Wisconsin, USA; [2]Department of Biology, Austin Peay State University, Clarksville, Tennessee, USA; [3]Mývatn Research Station, Skútustaðir, Iceland; [4]School of Art and Design, University of Oregon, Portland, Oregon, USA; [5]Arthur R. Marshall Loxahatchee National Wildlife Refuge, US Fish and Wildlife Service, Boynton Beach, Florida, USA; [6]Department of Biology, Creighton University, Omaha, Nebraska, USA

Abstract

Measuring microalgae density in soft-sediment benthos has challenges for even the most sophisticated methods. If the goal is to assess the photosynthetic potential of epipelon, then microalgae should be sampled only at the surface of the benthos to the depth of light penetration. Furthermore, microalgae density may show spatial and temporal variability that can only be captured by using many point samples and nondestructive sampling. Here, we use simple near-infrared (NIR) imagery to assess surface density of microalgae in soft underwater sediments and to infer their photosynthetic capacity. In lab studies, NIR imagery gives estimates of epipelon density that are strongly correlated with standard chlorophyll *a* (Chl *a*) assays using pigment extraction and fluorometry ($R^2_{adj} = 0.70$), but NIR imagery is better able to separate experimental treatments. In analyses of sediment samples from a lake, NIR imagery gives estimates of epipelon Chl *a* density that are strongly correlated to net ecosystem production (NEP). Near-infrared imagery also gives a fine-grained assessment of the spatial distribution of epipelon that helps to explain the relationship between epipelon density and NEP. Finally, images from an underwater NIR camera over the course of a wind disturbance event give estimates of the relative density of microalgae that is buried and is likely to be, at least temporarily, photosynthetically inactive. These results show that NIR imagery provides an easy and nondestructive method for sampling surface densities of microalgae which is particularly suitable for remote field locations and for educational settings in which students can generate results with cheap and robust equipment.

Assessing water quality and primary production in freshwater and marine ecosystems require a reliable proxy of microalgae abundance. For pelagic systems, the most widespread proxy is chlorophyll a (Chl *a*), which can be measured using a variety of methods (Holm-Hansen et al. 1965; Wetzel 2001). While it is not a perfect measure of phytoplankton density or photosynthetic activity (Jakobsen and Markager 2016; Wetzel 2001), the ease of assaying Chl *a* concentrations makes it a practical way to follow phytoplankton dynamics through time and compare phytoplankton densities among lakes, streams, and marine environments. In contrast to Chl *a* in pelagic systems, simple proxies for microalgae density and primary production face significant challenges in benthic systems, especially on soft sediment surfaces. This is a significant limitation given the growing recognition that benthic primary production can be an important contributor

*Correspondence: arives@wisc.edu

Associate editor: Hongsheng Bi

Data Availability Statement: Code and data are available open access (https://doi.org/10.6084/m9.figshare.26790517)

to the overall primary production of lakes and estuarian systems (Hope, Paterson, and Thrush 2020; Vander Zanden and Vadeboncoeur 2020).

The challenges for developing a reliable proxy for epipelon density and production in sediments arise because sediments have both vertical and horizontal structures. Soft sediments are often disturbed by abiotic and biotic forces, which bury microalgae below the sediment surface (Jacobs et al. 2021). While buried cells may survive and even accumulate nutrients while buried, they cannot be photosynthetically active where light does not penetrate. Therefore, only microalgae densities on the sediment surface determine the immediate role of the benthos in primary production (Jesus et al. 2014). The vertical structure of the sediment creates a challenge for sampling methods to select only the photosynthetically active surface of the sediment. Furthermore, many benthic microalgal species are motile, so that the photosynthetically active component of the epipelon community may vary with the factors that determine algal movement and orientation (Kromkamp, Morris, and Forster 2020). Epipelon communities are also spatially and temporally variable (Androuin et al. 2018; Chapman et al. 2010; Chennu et al. 2013, 2015; Jesus et al. 2014; Koh et al. 2007), and horizontal spatial variation in densities can occur on the scale of millimeters to meters. Finally, temporal variation requires nondestructive sampling so that changes in epipelon densities can be monitored in the same location.

We were confronted with these challenges in our study of Lake Mývatn, Iceland, a shallow naturally eutrophic lake in which benthic production exceeds pelagic production except during late summer in years when there are pelagic cyanobacterial blooms (Einarsson et al. 2004; McCormick et al. 2021). The epipelon community is primarily made up of diatoms, both colonial (e.g., *Fragilaria* spp.) and single-celled species (e.g., *Cymbella* spp.), some of which are motile (e.g., *Surirella* spp.) (Einarsson et al. 2004; McCormick, Phillips, and Ives 2019). The lake floor is covered by a meters-thick layer of diatomaceous ooze which is highly susceptible to wind disturbance; we have observed sediment mixing to a depth of over 5 cm during windstorms. To characterize spatial and temporal variation in epipelon, we have used chlorophyll extractions and measurements of net ecosystem production (NEP) under light saturating conditions on sediment collected using Kajak corers (Fig. 1a) (Ives 2021). Chlorophyll extractions illustrate the challenges of measuring epipelon densities. First, microalgae occur at high densities in sediment to depths of several centimeters, which we can show by slicing cores and extracting Chl *a* at different depths for fluorometric analyses. Second, estimates of Chl *a* and NEP may vary several-fold among cores taken within meters of each other, implying spatial variation in epipelon and photosynthetic potential at the scale of meters. We also use lab experiments to investigate algal and midge (Diptera: Chironomidae) growth under different experimental conditions. These experiments show spatial variation at finer scales: the midge larvae spin silk tubes from which they feed, creating variation in microalgae communities

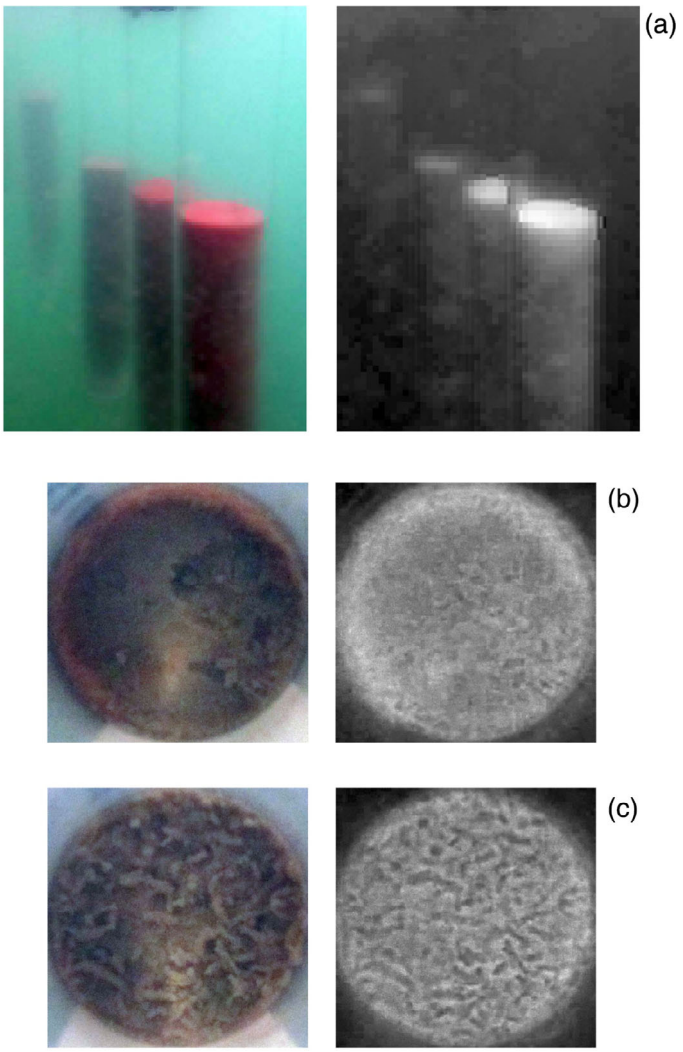

Fig. 1. Examples of near-infrared (NIR) images (left) and an index of microalgae density, BGN_NDVI (right). (**a**) Kajak sediment cores are used to estimate net ecosystem production (NEP) by incubating them for 3 h suspended at a depth of 0.5 m in Mývatn; cores in black tubes used to estimate respiration have been removed. The NIR image was taken at our central station (Sta. 33) during our routine monitoring using standard protocols (Ives 2021). Kajak cores are 0.5 m long and 5 cm in internal diameter. Note that the decreasing NIR reflectance (shown as red) with more distant cores is due to water turbidity and low water transparency to NIR radiation. (**b**, **c**) Experimental tubes (3 cm in diameter) without (**b**) and with (**c**) added midges that form silk tubes. The images were taken after 22 d in a growth chamber.

at the scale of millimeters (Fig. 1b,c). This fine-scale variation may affect NEP by creating small areas with high or low microalgae densities which lead to microscale nutrient limitation.

Three general methods are available for in situ measurement of proxies of microalgae densities on underwater surfaces (Kromkamp et al. 2006; Kutser et al. 2020). Field fluorometers use the excitation and emission frequency of pigments to give optically specific measurements of the concentration of Chl *a* in benthic microalgae (Bertone, Burford, and Hamilton 2018;

Kromkamp, Morris, and Forster 2020; Stock et al. 2019). By separately measuring taxonomically specific pigments, fluorometers can also give gross taxonomic composition of a sample, separating for example diatoms, cyanobacteria, and chlorophytes. Standard fluorometry requires shielding from external light sources which limits use on soft sediments that are disturbed when touched. Pulse–amplitude–modulation fluorometry overcomes this limitation by allowing natural light sources (Maggi et al. 2013) and also gives a more-direct measure of photosynthetic activity tied to the efficiency of photosystem II (Daggers et al. 2018; Huot and Babin 2011). Nonetheless, standard and Pulse–Amplitude–Modulation fluorometers measure averages over illuminated (excited) surfaces and therefore require repeated measurements to characterize spatial variation.

Hyperspectral imaging measures the reflectance of samples in many narrow bands from near-infrared (NIR) to ultraviolet wavelengths, and field-deployed hyperspectrometers have been developed for underwater work with either artificial or natural light sources (Dumke et al. 2018a; Ghunowa, Medeiros, and Bello 2019; Kazemipour, Méléder, and Launeau 2011; Kromkamp et al. 2006; Mogstad, Johnsen, and Ludvigsen 2019; Montes-Herrera et al. 2021; Murphy et al. 2005; Murphy and Underwood 2006). Using the spectral reflectance from benthic microalgae, hyperspectrometers can estimate Chl *a* densities. Hyperspectral imaging can also characterize the taxonomic composition of samples using algorithms that separate the spectral signatures of different pigments, although this requires calibration against the spectral signatures of the component taxa in the specific microalgae community (Barillé et al. 2017; Dumke et al. 2018b; Jesus et al. 2014; Russell et al. 2016). A limitation of hyperspectral imaging is light availability needed to record reflectance at many wavelengths; a single image may require 10 min to capture using a specialized motorized frame (Chennu et al. 2013). Newer technologies, however, allow mounting hyperspectral cameras on remotely operated vehicles (Summers et al. 2022).

The third approach to measuring microalgae density in benthic communities is near infrared (NIR) imaging (Daggers et al. 2018; Kromkamp et al. 2006; Murphy, Underwood, and Jackson 2009; Zhang et al. 2021). In contrast to hyperspectral imaging, NIR imaging uses only two or three spectral bands that are combined to give a simple index of microalgae density (O'Reilly and Werdell 2019; Tong et al. 2022). For example, the well-known normalized difference vegetation index (NDVI) requires NIR and red wavelengths, using the high reflectance of Chl *a* in NIR as the signal and red as the reference to represent the overall reflected light levels (Tucker 1979). Near-infrared imaging has been used for benthic and intertidal estuarian sediments either with modified commercial cameras (Murphy et al. 2004) or by tricking unmodified cameras to take images in the NIR (Murphy, Underwood, and Jackson 2009). Although it lacks the potential of fluorometry and hyperspectrometry to separate pigments and therefore indicate the relative composition of the microalgae community, NIR is simple and uses inexpensive equipment. Therefore, it gives a method for measuring benthic microalgae density that is comparable in ease to fluorometric measurements of Chl *a* as a proxy for phytoplankton density in the pelagic zone.

Here, we validate and illustrate the use of NIR imagery as a proxy of microalgae density on soft sediment surfaces both in lab and field settings. First, we present three experimental lab studies to compare the results derived using estimates of epipelon density obtained from NIR imagery to those obtained by extracting Chl *a* from samples using methanol and measuring Chl *a* by standard fluorometric methods. Second, we report on two studies in which we measured NEP as the rate of dissolved oxygen evolution. We then tested whether our NIR measure of epipelon density was correlated with NEP. One of these studies was performed with a manipulation of midge larvae presence/absence (Fig. 1b,c), making it possible to assess NIR imaging as a tool to investigate fine-scale spatial variation in microalgae density. Finally, as an illustration of the types of information that NIR imagery can provide from the field, we mounted a NIR camera above the sediment surface in Lake Mývatn which took photos every 2 min. During one day of this deployment, there was a short wind event that disturbed the sediment surface. We use NIR images before, during, and after the disturbance to estimate how much of the photosynthetically active microalgae community on the surface was buried in the windstorm.

Materials and procedures

Cameras

We have used three cameras: a Canon Powershot, a GoPro HERO4, and a GoPro HERO7. All cameras had their red channel converted to NIR (850 nm), the Canon Powershot by Llewellyn Data Processing (maxmax.com) and the GoPros by Kolari Vision (kolarivision.com). For our needs, GoPros are the more versatile because they have a wide focal distance, and the HERO7 is waterproof. Converted GoPros can be purchased for under US$600. To monitor changes in the benthos, we mounted the GoPro HERO4 in a waterproof camera box with additional lithium batteries that allow taking time-lapse images for several months using a Blink Time Lapse Controller (CamDo, https://cam-do.com). The camera assembly was attached to a 50 × 50-cm aluminum frame at 30 cm above the sediment surface facing downward.

BGN_NDVI

The index we used as the proxy for microalgae density is

$$\mathrm{BGN\_NDVI} = \frac{\mathrm{NIR} - 0.5(\mathrm{G} + \mathrm{B})}{\mathrm{NIR} + 0.5(\mathrm{G} + \mathrm{B})}$$

where G and B are green and blue optical channels. This is similar to NDVI but with the term 0.5(G + B) replacing R, the red channel. Values of NIR, G, and B range between 0 and 1,

and therefore BGN_NDVI ranges between −1 and 1. Our rationale for using BGN_NDVI is that the light source penetrating to the benthos is filtered through water, which favors the blue spectrum, and light is further filtered through phytoplankton; the water is blue-green. Furthermore, diatoms are the dominant benthic algae at Mývatn, and carotenoids that give diatoms their golden-brown color have absorbance peaks at longer wavelengths (G) than Chl *a* (B). These factors argue for using 0.5(G + B) as the reference against which NIR is compared. We compared BGN_NDVI with other indices that we could compute using the B, G, and NIR bands that were available on our cameras, and of these, the indices using NIR as the main signal of microalgae density were highly correlated (Supporting Information section "Additional indices of Chl a from reflectance").

Because NIR imagery measures reflectance, the light source will affect the quantitative results. Therefore, we generally use NIR imagery as a proxy for relative rather than absolute microalgae densities. In laboratory settings, we use indirect sunlight in situations when we can take a single image of all experimental replicates we want to compare. When this is not possible, we take images of individual replicates using a controlled light source given by a 60-W incandescent bulb; incandescent bulbs are strong emitters of NIR as well as visible light. Images are taken using a simple frame with a light diffuser that maintains a standard distance between the replicate and the bulb. Repeatability of image values is high using this setup.

Although we refer to BGN_NDVI as a measure of microalgae density, we emphasize that it is a standardized measure of NIR reflectance. Thus, it is less specific to Chl *a* than measurements obtained using standard fluorescence methods on extracted sediment samples. A further advantage of extraction and fluorescence is that this gives "corrected" Chl *a* concentrations after accounting for the concentration of pheophytin *a*, a breakdown product of Chl *a* (Arar and Collins 1997). The relative concentrations of pheophytin *a* to Chl *a* can itself be a useful indicator of algal cell death and breakdown.

We processed images using the jpeg package (Urbanek 2022) in the R programming language (R Core Team 2023). Code and data are available open access (https://doi.org/10.6084/m9.figshare.26790517).

Experimental comparison of NIR imagery and Chl *a* estimated with fluorometry

To compare NIR imagery to the standard approach of extracting Chl *a* and using fluorometry, we performed three experiments designed to generate a range of epipelon density. The experiments were intended to give the best fluorometric estimates of benthic Chl *a* densities that then serve as a standard against which to evaluation NIR imagery. All experiments were performed at the Mývatn Research Station, Iceland, which has limited lab equipment.

In the first experiment, 18 microcosms were constructed from 50-mL centrifuge tubes (3 × 11 cm) by cutting the bottoms off and inverting so that sediment could be added to the bottom. Fine 20-μm mesh was placed as a barrier 1.5 cm above the bottom of the inverted tubes to prevent the movement of motile diatoms. On 01 September 2017, the bottoms of the 18 tubes were filled with surface sediment (top 1.5 cm) taken from 18 Kajak cores, 3 from each of 6 permanent sampling sites that we have at Mývatn. We expected that sediment from cores at different sites would differ in nutrient content and therefore be of differing quality for algal growth. Filters (Whatman GF/A) were placed on top of the mesh and inoculated with a dilute aliquot of homogenized sediment from the top 1.5 cm of sediment collected from one of the sites and filtered through 125-μm mesh. Six additional tubes were set up without sediment and therefore had no nutrients beyond those available in the spring water used to fill the tubes. Tubes were placed in a refrigerator at ∼ 10°C and illuminated with saturating photosynthetically active radiation (PAR) light (∼ 100 μmol m^{-2} s^{-1}). After 24 d, filter papers were removed, spread on a damp paper sheet, and imaged together with the Canon Powershot under indirect sunlight. The filters were then frozen separately. Twenty-four hours before fluorometry, filter papers were placed in 20 mL methanol at 4°C, and fluorescence was measured with an Aquafluor (Turner Designs) using standard protocols (Ives 2021). "Corrected" Chl *a* was computed by subtracting the fluorometric values after acidifying samples with 0.1 N HCl; the corrected Chl *a* measurements remove the fluorometric signal of pheophytin *a* (Arar and Collins 1997). The Aquafluor is factory-calibrated in units of μg Chl *a*/L. In summary, the experiment measured the growth of a common inoculum on filter paper, with sediment below the mesh providing variation in nutrient availability for the growth of the common inoculum, and final measurements were made with both NIR imagery and fluorescence.

The second experiment used the same microcosms, but nutrient additions were used to create differences in epipelon density. On 23 May 2018, the bottoms of 32 tubes were filled with homogenized sediment taken from the top 8 cm of Kajak cores from our central sampling site at Mývatn (Sta. 33). We added nutrients in a 2 × 2 × 2 design for ammonium, phosphate, and silicate with each treatment replicated 4 times. Ammonium (NH_4Cl) and phosphate (KH_2PO_4) were added for final concentrations of 400 and 50 μM L^{-1}, which are the highest concentrations measured at a depth of 1 cm in Mývatn sediment (Anon 1991). Silicate ($H_{18}Na_2O_{12}Si$) was added at 800 μM L^{-1}, which is roughly the average concentration found in springs that feed Mývatn. Filter paper on top of the 20-μm mesh was inoculated with a diluted and homogenized sample from the top 1.5 cm of the sediment. An additional three tubes were included that were not inoculated nor given nutrients, but included bottom sediments. Tubes were placed in a refrigerator at ∼ 10°C with saturating actinic light (∼ 60 μmol m^{-2} s^{-1}, measured with a PAR light meter) for 8 d, and then NIR images and fluorescence measurements were taken as in the first experiment. In summary, the experiment

measured the growth of a common inoculum on the filter paper with nutrients diffusing from sediments and with variation in growth created by nutrient additions.

The third experiment used similar microcosms made from 50-mL centrifuge tubes, but no mesh or filter paper was used. Therefore, they give the realistic case of microalgae growing directly on sediment. Sediment was collected on 18 August 2020, from the top 0.5 cm of Kajak core samples from our central sampling location in Mývatn, and simultaneously water was collected from above the sediment. Sediment was homogenized by sieving through 250-μm mesh and then distributed among 24 tubes to a depth of 0.5 cm, with lake water added for a total volume of 20 mL. Treatments were implemented in a 2 × 2 experimental design for full light/shading and ammonium addition/control at the same concentrations as the second experiment. Near-infrared images of the tubes were taken on days 3, 6, and 13 of the experiment with the GoPro HERO4 using an incandescent light source, and after the final NIR images each tube was fluorometrically assayed for Chl *a* by vigorously resuspending sediment, taking a 1-mL sample, extracting Chl *a* in 10 mL methanol for 24 h, and performing fluorometry using our standard protocol. This third experiment used the ability of NIR imagery to sample for microalgae density nondestructively and hence repeatedly over the course of an experiment; at the end of the experiment, we compared NIR imagery with fluorometry obtained destructively.

Comparison of NIR imagery and NEP

To determine whether NIR imagery estimates of epipelon density could predict NEP, we used two experiments (fourth and fifth experiments).

In the fourth experiment, we reconstructed sediment cores in centrifuge tubes and measured BGN_NDVI and NEP. To generate variation among tubes, we used three sediment samples taken with a Kajak corer on 13 June 2023, from each of our 6 permanent sampling sites in Mývatn, and to assess the repeatability of measurements, we created 2 replicates from each of the 18 sediment samples. For one replicate, we filled a tube with 20 mL of sediment taken from the Kajak core at a depth of 8–12 cm. For the second replicate, we filled a tube with 20 mL of clean sand. We then added 4 mL of inoculum made from a homogenized sample of the top 0.75 cm of the Kajak core in both tubes. Thus, top sediment from each of the 18 Kajak core samples was placed in two tubes, with one tube containing bottom sediment and the other containing sand. Because the measurements we present were taken in the first 24 h, we did not expect to find a difference between tubes with bottom sediment and sand; this was the first part of a long-term bioassay we use to assess variation in nutrient flux from sediments to benthic algae. We placed all tubes in a refrigerator with saturating actinic lights. After 24 h we took NIR images with the GoPro HERO7 of each chamber using an incandescent light source. We then measured dissolved oxygen (DO) with an optical DO probe (ProODO, YSI). We computed NEP from the DO concentration under the assumption that the DO concentration was at steady state between NEP from the algae in the sediment and flux to the atmosphere (*see* Supporting Information section "Measuring NEP using open containers").

The fifth experiment was designed to measure the effect of midge (Chironomidae: *Tanytarsus gracilentus*) larval presence on microalgae growth, and microalgae growth on larval growth and development rates (Botsch et al. 2023). The experiment was conducted in August 2020 and crossed the presence/absence of midge larvae with a gradient in initial density of microalgae. The gradient consisted of 10 microalgae densities created by serially diluting sediment from the top 0.5 cm of Kajak cores taken from our central sampling location at Mývatn with microalgae-poor sediment collected from 5 to 10 cm depth. Five replicates were produced for each of the 20 treatments, and 2 and 3 replicates were sampled on days 14 and 22, respectively; here we present data from the 60 experimental tubes sampled on day 22 when midge larvae had more time to affect microalgae. We took NIR images using an incandescent light source. Then, NEP and ecosystem respiration were estimated by measuring DO concentrations, capping the tubes, incubating them in the light (24 h) or dark (11 h), and re-measuring DO concentrations. In contrast to the fourth experiment which measured DO concentrations in unsealed containers, the procedure using capped containers allowed the separation of gross ecosystem production, NEP, and ecosystem respiration. In addition to calculating the mean BGN_NDVI for each experimental tube, we computed the "grain" or spatial scale of variation in BGN_NDVI: we divided the images into 189 64 × 64 pixel grids, averaged the BGN_NDVI within each grid, calculated the standard deviation among grids, and divided by the standard deviation in BGN_NDVI calculated from all 656,989 pixels. When this measure of grain is low, much of the variation in BGN_NDVI occurs within the 64 × 64 pixel grids, and therefore lower values represent more fine-grained spatial variation. We also investigated other measures of spatial variation (*see* Supporting Information section "Spatial variation caused by midges in a lab experiment"). A complete description of the experiment is given in Botsch et al. (2023), although values of BGN_NDVI were not included.

The fourth and fifth experiments apply NIR imagery in situations that would be difficult for Chl *a* extraction and fluorometric measurement. In the previous experiments that used filter paper (first and second lab experiments), it was possible to get good samples of the growing community of algae for fluorometry. In the previous experiment that used sediment (third lab experiment), a thin layer of sediment was used so that the entire sample could be resuspended and sampled for fluorometry. In the fourth and fifth experiments, only at the top of the sediment will there be enough light penetration for photosynthesis, and there is no easy method for assaying only the photic sediment zone. Therefore, we did not perform fluorometry.

Field deployment of NIR imagery

We used the GoPro HERO4 mounted on a frame to monitor changes in the benthos from 16 June 2023 to 19 June 2023, in which images were taken every 2 min. During the daylight hours on 18 June 2023, the average windspeed was 18 km h^{-1}, although there was a period of 27 km h^{-1} around 13:00–15:00, with gusts to 40 km h^{-1}. We present images from before, during, and after the effects of this gusty period.

Assessment

Below, we first present the results from experiments to compare epipelon densities assessed using NIR imagery (BGN_NDVI) to Chl *a* measured by fluorometry in laboratory situations that should allow accurate fluorometry measurements. We then use results from two experiments to assess the ability of NIR imagery to predict NEP, which should be closely associated with microalgae density under laboratory conditions. Finally, we take advantage of two features of NIR imagery—the ability to take nondestructive samples and sample an entire 2D surface—to quantify the effect of a wind disturbance on the burial of microalgae on the sediment surface of Mývatn.

Experimental comparison of NIR imagery and fluorometry

We performed three lab experiments to compare BGN_NDVI values to those obtained by extracting Chl *a* with methanol and measuring Chl *a* using fluorometry. In the two experiments in which a common inoculum was grown on filter paper, there was a strong relationship between BGN_NDVI and Chl *a* from fluorometry (Fig. 2). In the first experiment (Fig. 2a) the regression of BGN_NDVI on Chl *a* from fluorometry was highly significant ($t = 6.85$, $p < 0.00001$) with $R^2_{adj} = 0.70$. Although it appears that there might be a saturating effect at high BGN_NDVI, a quadratic term in a polynomial regression was not significant ($t = -1.68$, $p = 0.11$). In the second experiment (Fig. 2b), the regression of BGN_NDVI on Chl *a* excluding the non-inoculated filter papers was highly significant ($t = 8.37$, $p < 0.00001$) with $R^2_{adj} = 0.69$. In the third experiment (Fig. 2c), no filter paper was used, and measurements were taken directly on sediments: NIR images were taken of the surface of the 0.5-cm-thick sediments, and Chl *a* was extracted with methanol from the sediment after resuspension. The relationship between BGN_NDVI and Chl *a* from fluorometry at the end of the experiment was weaker than in the first two experiments, with a moderately significant slope ($t = 2.49$, $p = 0.032$) and $R^2_{adj} = 0.32$.

The second experiment had a 2 × 2 × 2 factorial design with ammonium (N), phosphate (P), and silicate (Si) additions, making it possible to ask whether BGN_NDVI or Chl *a* from fluorometry was better able to identify a treatment effect (Table 1; Fig. 3). BGN_NDVI identified a significant main effect of N and a N : Si interaction, with an overall $R^2_{adj} = 0.52$. In contrast, Chl *a* from fluorometry failed to detect any treatment effects and had an $R^2_{adj} = 0.31$. We also analyzed the "uncorrected Chl *a*" obtained from fluorometry before acidification. The uncorrected Chl *a* contains fluorescence from pheophytin *a* and therefore might give more similar measurements to BGN_NDVI. The regression using uncorrected Chl *a* identified a main effect of N and had an $R^2_{adj} = 0.38$. The regression of BGN_NDVI on uncorrected Chl *a* ($R^2_{adj} = 0.72$) was also slightly stronger than on corrected Chl *a* ($R^2_{adj} = 0.69$, Fig. 2b).

The third lab experiment had a 2 × 2 factorial design with treatments for shade and saturating light (S and L), and ammonium addition and control (N and C). Near-infrared

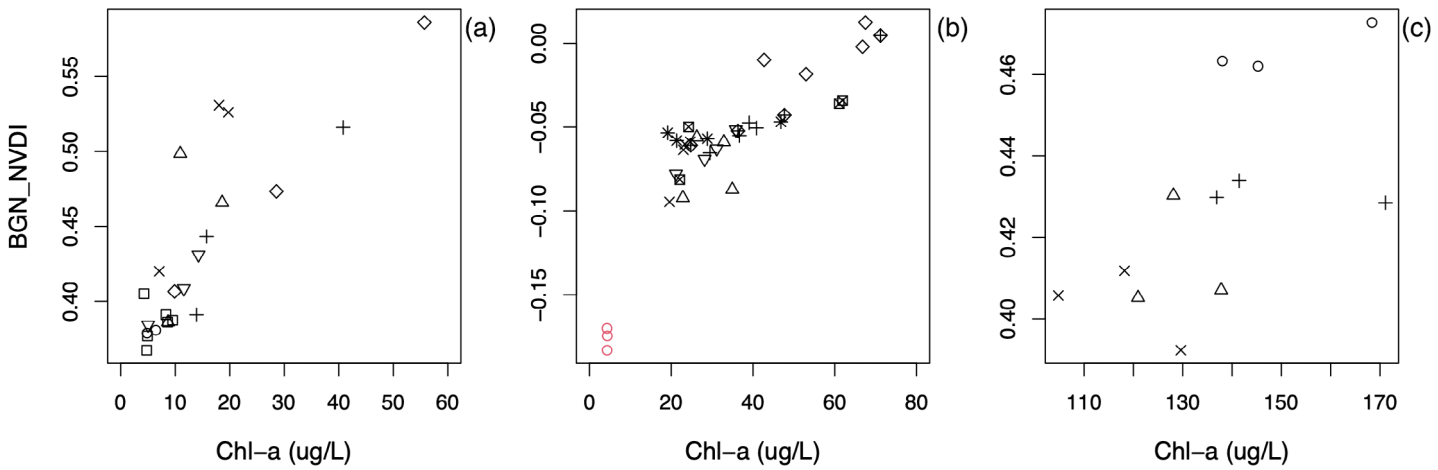

Fig. 2. Three lab experiments comparing epipelon density estimated from BGN_NDVI and from fluorometry. (**a**) In the first lab experiment, filters were placed above sediment collected from six lake sites (symbols). (**b**) In the second experiment, filters were inoculated with a common sediment stock and nutrients were added in a 2 × 2 × 2 factorial design of presence/absence of ammonium, phosphate, and silicate (symbols); in addition, there were three replicates without sediment underneath the filters (red circles). (**c**) The third experiment had a 2 × 2 design crossing light level with ammonium addition (symbols), and the data in the panel are from the last time point (day 13) of the experiment.

Table 1. ANOVA results from the second lab experiment showing the abilities of different measures to detect experimental treatment effects (*see* Fig. 3). The experiment had a 2 × 2 × 2 factorial design for addition of ammonium (N), phosphate (P), and silicate (Si). BGN_NDVI was measured using near-infrared (NIR) imagery, and corrected chlorophyll a (Chl *a*) and uncorrected Chl *a* (including pheophytin) were measured using fluorometry. The no-inoculum control was excluded from the statistical analyses.

		BGN_NDVI		Chl *a*		Uncorrected Chl *a*	
Treatment	df	*F*-value	*p*-value	*F*-value	*p*-value	*F*-value	*p*-value
N	1	7.536	0.011*	2.927	0.100	5.138	0.032*
P	1	1.993	0.170	0.002	0.963	0.142	0.710
Si	1	3.113	0.090	0.590	0.450	1.100	0.304
N : P	1	3.380	0.078	2.755	0.109	2.123	0.158
N : Si	1	4.301	0.049*	0.503	0.485	0.933	0.343
P : Si	1	1.430	0.243	0.417	0.524	1.108	0.303

imagery allowed repeated nondestructive measurements of the sediment surface on days 3, 6 and 13, after which sediment was resuspended and Chl *a* extracted and measured with fluorometry (Fig. 4). The repeated BGN_NVDI values show the establishment first of main effects of L and N treatments (day 6), followed by the emergence of an interaction effect (day 13). On day 13, NIR imagery revealed negative main effects of L ($t = -4.700$, $p = 0.0015$) and N ($t = -6.90$, $p = 0.00012$), and a marginally significant positive L : N interaction ($t = 2.29$, $p = 0.051$). In contrast, fluorometry did not reveal any significant treatment effects, although there was a negative nonsignificant effect of N. An increase in BGN_NVDI at low light (S) can be biologically explained if the benthic algae increase their investment in Chl *a* to compensate. The strong negative effect of N on BGN_NVDI is biologically more difficult to explain and was not found in similar experiments such as the second experiment in which N had a positive effect (Table 1). Nonetheless, response of NEP to the N treatment on day 13 was also negative ($t = -8.198$, $p < 0.00001$), consistent with the effect on BGN_NVDI.

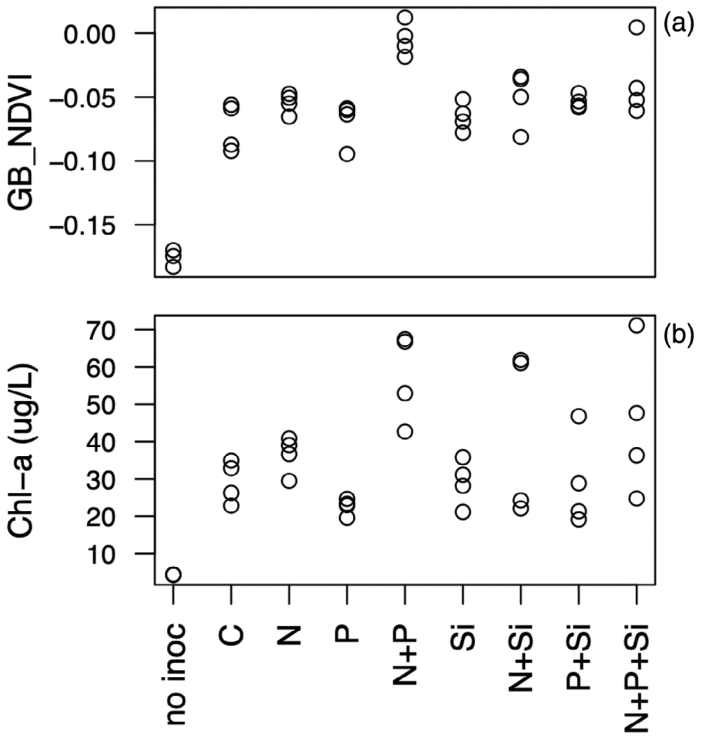

Fig. 3. The second lab experiment (Fig. 2b) compared the results obtained using measures to detect experimental treatment effects (*see* Table 1). The experiment had a 2 × 2 × 2 factorial design for addition of ammonium (N), phosphate (P), and silicate (Si). BGN_NDVI was measured using near-infrared (NIR) imagery, and Chl *a* was measured using fluorometry.

Comparison of NIR imagery and NEP

In the fourth experiment performed on sediment samples collected from six locations in Mývatn, there was a strong relationship between BGN_NVDI and NEP (Fig. 5; $t = 10.8$, $p < 0.00001$, $R^2_{adj} = 0.77$). In the experimental design, sediment from three Kajak cores at each site (18 total cores) were divided in half, and two replicates were created that were different only in the substrate (sediment vs. sand) on which the samples were placed. This makes it possible to compare repeated BGN_NDVI measurements on replicates of the same samples. Partitioning the variance of BGN_NDVI among the 36 samples, the variance due to differences among BGN_NDVI measured from the same sample was 16% of the total variance. This repeatability estimate includes not only variation in the measurement of BGN_NDVI, but also variation in the construction of the replicates. A similar partitioning of variances in NEP showed greater repeatability, with the variance due to differences among replicates equal to 3% of the total variance. The higher repeatability of NEP than BGN_NDVI suggests that measurement error of BGN_NDVI is greater than NEP.

In the fifth experiment, a statistical model including BGN_NDVI and presence/absence of midge larvae gave a strong relationship with NEP (Fig. 6a; BGN_NDVI, $t = 7.897$,

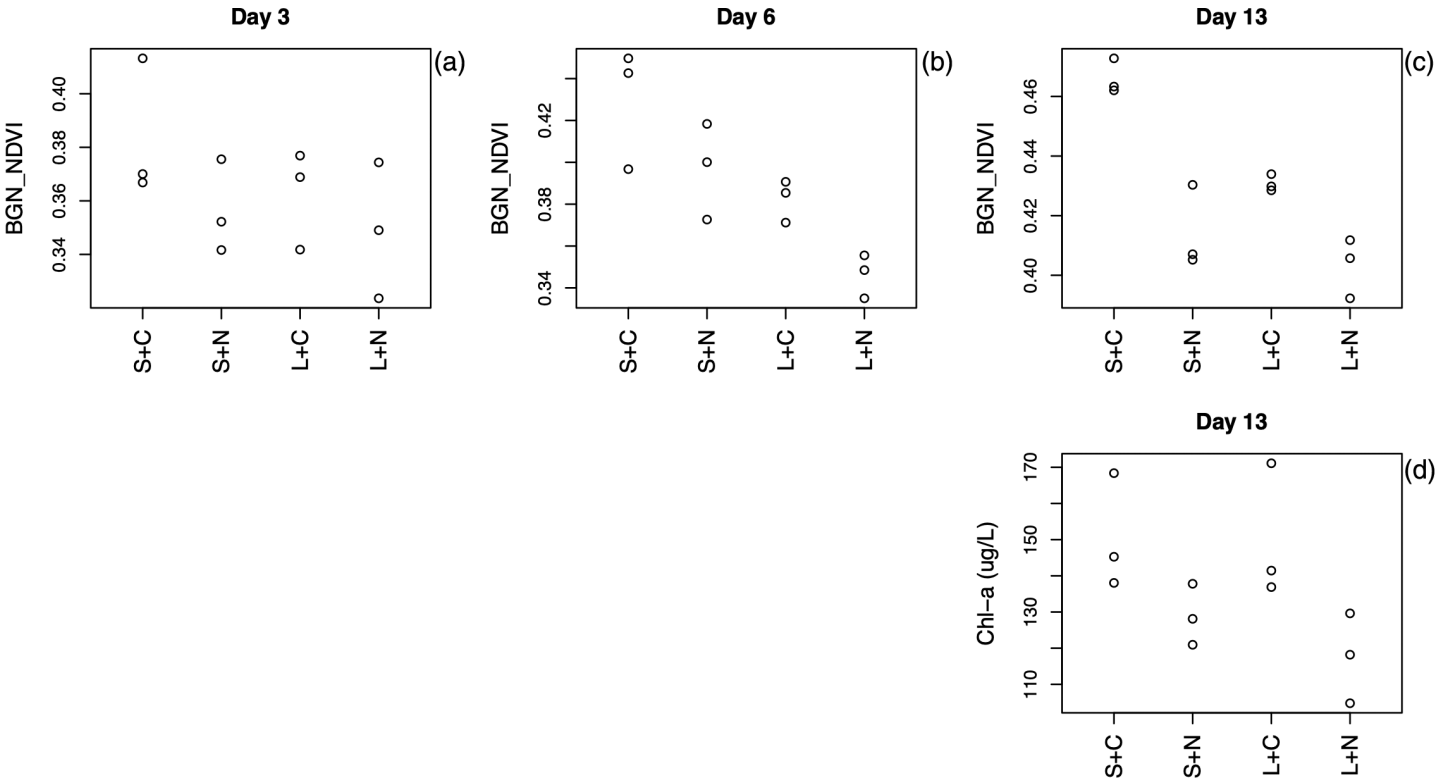

Fig. 4. The third lab experiment (Fig. 2c) used repeated near-infrared (NIR) imaging to reveal changes in relative BGN_NDVI on surface sediments (**a**–**c**), and at the end of the experiment sediment was resuspended and sampled for fluorometric determination of Chl *a* (**d**). Treatments are shaded (S) and saturating light (L), and control (C) and ammonium addition (N).

$p < 0.00001$; midges, $t = 4.695$, $p = 0.00002$; $R^2_{adj} = 0.65$). For a given value of BGN_NDVI, the presence of midge larvae decreased NEP. A possible explanation for this, that replicates with midges had higher ecosystem respiration, can be ruled out because replicates without midge larvae had generally higher ecosystem respiration than those with larvae (Supporting Information Fig. S4a). A second explanation is that replicates with midge larvae had higher fine-grained variation in epipelon densities which affected NEP; for example, high variation in epipelon densities could lead to localized competition for nutrients and reduced overall NEP. The spatial grain in epipelon as determined by BGN_NDVI was finer in the presence of midge larvae in replicates with low mean BGN_NDVI (Fig. 6b). The replicates with low mean BGN_NDVI (e.g., Fig. 1c) were those that had low epipelon densities at the start of the experiment and therefore were influenced more by the presence of midge larvae (Botsch et al. 2023).

Field deployment of NIR imagery

The field deployment of an NIR camera revealed the effect of a wind disturbance to bury microalgae under the sediment surface (Fig. 7). Around 13:30 on 18 June 2023, water currents were strong enough to disturb the sediment surface, resulting in a decrease in BGN_NVDI. The decrease was roughly one standard deviation of the distributions of values among pixels within images. Although BGN_NDVI does not give absolute densities of Chl *a*, if the lowest value of BGN_NVDI within a pixel is assumed to represent zero (no epipelon), then the wind disturbance decreased the density of microalgae exposed to light by 30–40%. This represents a maximum estimate of the decrease in epipelon density, because even the pixel with the lowest BGN_NVDI value might have contained epipelon. Nonetheless, the magnitude of the decrease in BGN_NVDI suggests a large impact of the wind disturbance. Note also that before and after the wind disturbance, the mean values of BGN_NDVI were relatively stable, implying that changes in light conditions or other non-biological factors that could affect the values of BGN_NDVI through time are small compared to the spatial variation in BGN_NDVI values within images (*see* Supporting Information section "Field deployment and alternative formulations of BGN_NDVI").

Discussion

The results show that NIR imagery gives an effective nondestructive proxy for microalgae density on soft sediment that can be used in both the lab and field. We performed three lab experiments designed to calibrate NIR imagery against fluorometric measurements of Chl *a* using designs for which we

thought fluorometry would be a good standard. For epipelon communities grown on filter paper from which Chl *a* could be easily extracted, there was a strong association between BGN_NDVI from NIR imagery and Chl *a* from fluorometry (Fig. 2). While we used fluorometry as the standard, the second experiment gave evidence that NIR imagery was outperforming fluorometry (Fig. 3): BGN_NDVI explained more variation among experimental treatments than fluorometry (Table 1). In the third lab experiment using sediment rather than filter paper, the association between NIR imagery and fluorometry was less tight (Fig. 2c), and BGN_NDVI was again able to detect treatment effects that fluorometry did not (Fig. 4). These experiments left us with greater confidence in NIR imagery than fluorometry for estimating microalgae density at the surface of soft sediment.

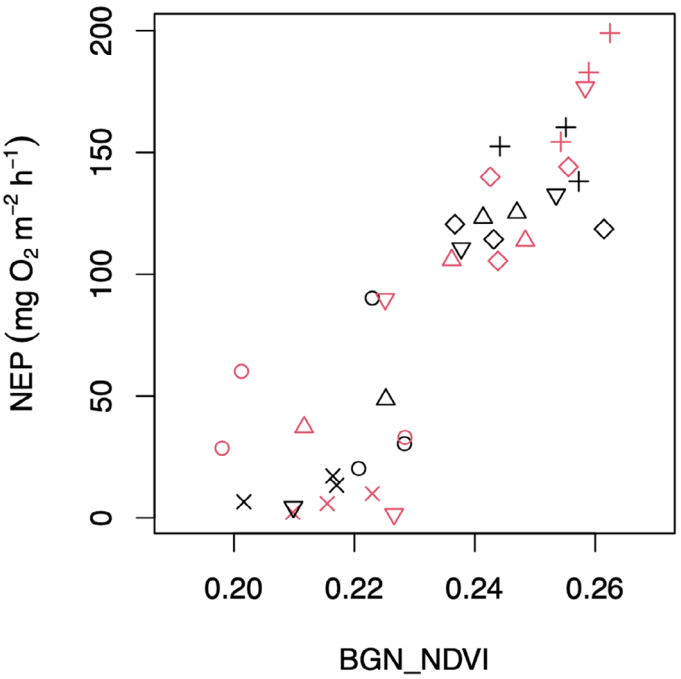

Fig. 5. The fourth experiment allowed a comparison between net ecosystem production (NEP) and BGN_NDVI. Eighteen sample Kajak cores from six sampling locations in Mývatn (different symbols) were split between two tubes and placed above either sediment (red symbols) or sand (black symbols). Tubes were then placed in a growth chamber at saturating actinic light levels for 24 h, after which near-infrared (NIR) images were taken.

BGN_NDVI was also a strong predictor of NEP in sediment samples taken from the field (Figs. 5,6). Because NIR imagery measures reflectance only to the depth of light penetration, which for sediments is generally less than 2 mm (Cartaxana et al. 2011; Gomoiu 1967; Kühl, Lassen, and Jorgensen 1994), it measures the density of microalgae that are exposed to light (Jesus et al. 2014). Even though reflectance measures light that is not used for photosynthesis, for a light source of a given spectral composition, reflectance of NIR by epipelon should be roughly proportional to Chl *a*. We have investigated the fine vertical distribution of microalgae in the sediment by freezing minicores and examining slices at the millimeter scale. For sediments that are incubated under stable lab conditions, algal cells on the surface are more likely to be "living" (have expanded chloroplasts) and dividing, and strands of colonial species (*Fragilaria*) are longer. Therefore, in the lab the photosynthesis and growth of epipelon in response to experimental treatments is likely to be greatest on the sediment surface, which explains the close association between NEP and BGN_NDVI.

Near-infrared imagery also gives a simple means for assessing fine-scale horizontal spatial variation in epipelon density (*see* also Murphy, Underwood, and Jackson 2009). In our lab experiment on the effects of midge larvae on NEP, midge presence decreased the NEP within experimental

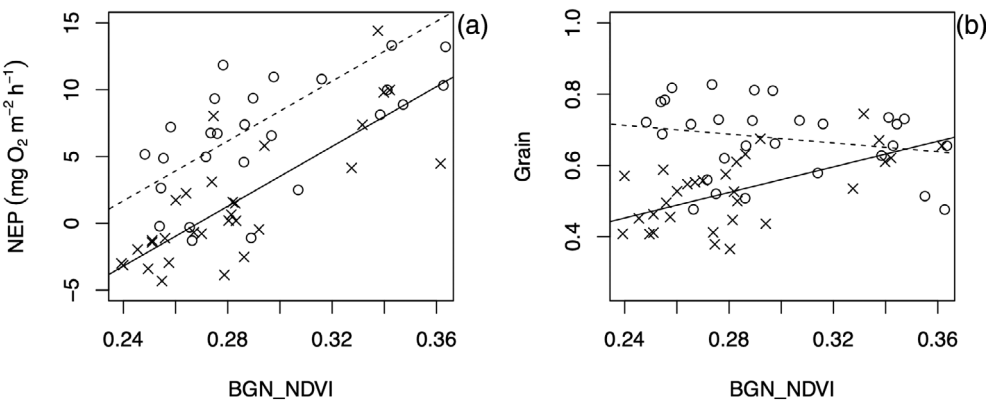

Fig. 6. Results from the fifth experiment varying the presence/absence of midge larvae with a gradient in initial epipelon density (10 levels) measured after 22 d (Botsch et al. 2023). (**a**) Estimates of net ecosystem production (NEP) for 30 replicates with (*x*'s and solid line) and without (o's and dashed line) midge larvae vs. BGN_NDVI. (**b**) Spatial grain of the variation in BGN_NDVI, with lower values implying finer grain (e.g., Fig. 1b has finer grain than Fig. 1c). Spatial grain was measured as the standard deviation of mean values of BGN_NDVI in 189 64 × 64 pixel grids divided by the standard deviation in values of BGN_NDVI for the 656,989 pixels per image.

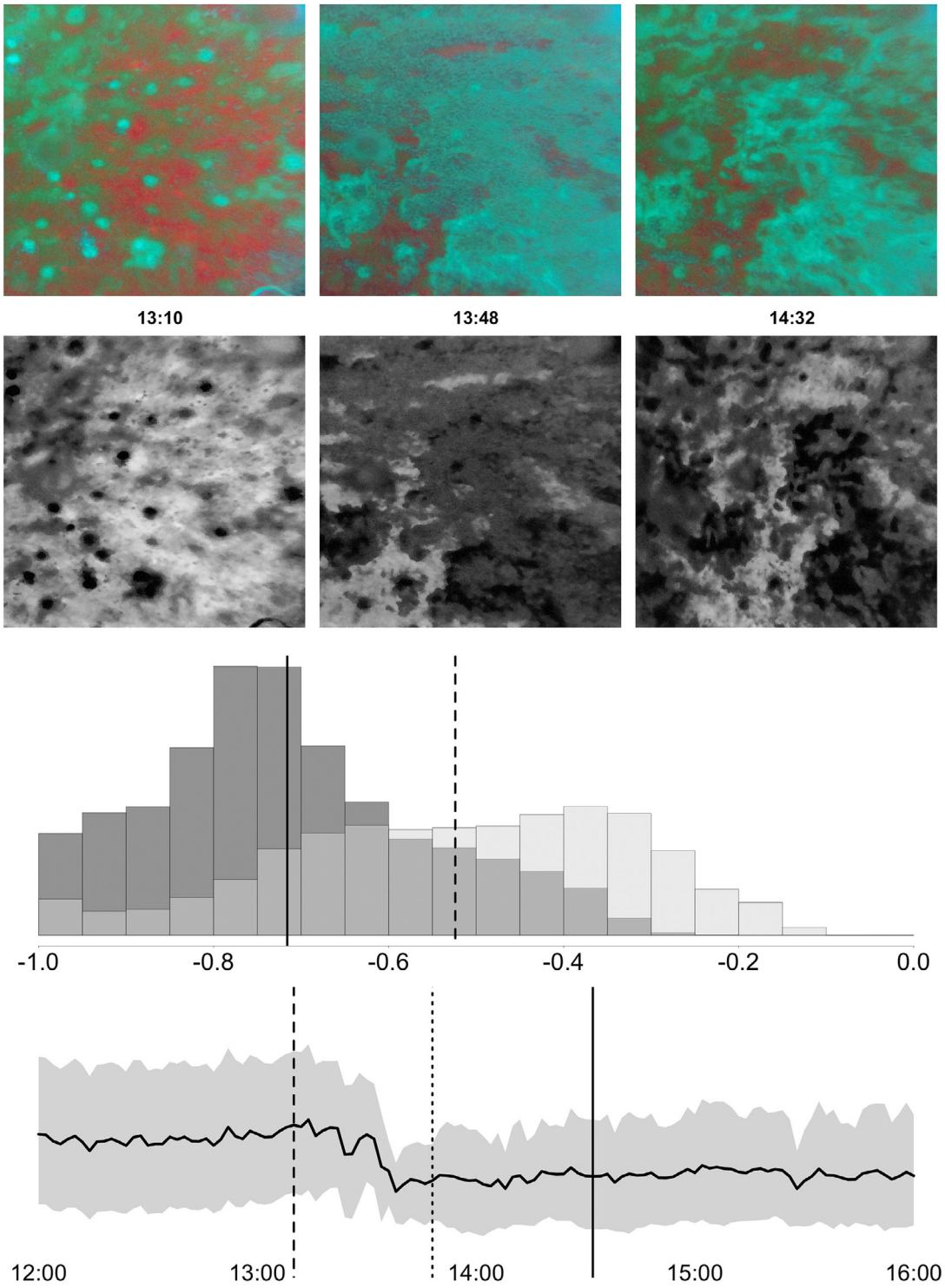

Fig. 7. Near-infrared (NIR) imagining was used to estimate the effect of a wind disturbance event on the density of epipelon exposed on the sediment surface of Mývatn on 18 June 2023. The top row shows images from 13:10, 13:48, and 14:32. The images were used to compute BGN_NDVI, in which higher BGN_NDVI is given in lighter shades of gray (second row). We suspect that the circular green areas (absence of epipelon) are the entrances of midge (*Chironomus islandicus*) tubes in the sediment based on samples from Kajak cores taken at the same time. The histograms show the distributions of BGN_NDVI from all pixels before (13:10, light gray) and after (14:32, black) the wind disturbance, with overlap between histograms shown in dark gray. Vertical dashed and solid lines give mean BGN_NDVI before and after disturbance. The lowest panel shows the time series of BGN_NDVI calculated from NIR images taken every 2 min; the shaded region gives the 68% inclusion intervals of BGN_NDVI values within the same image that are comparable to the standard deviation. Vertical dashed, dotted, and solid lines at 13:10, 13:48, and 14:32 correspond to the images at the top of the figure.

replicates for a given mean value of BGN_NDVI (Fig. 6a). A possible explanation is that midge larvae created fine-scale spatial variation in epipelon densities (Figs. 1b,c, 6b) which changed the relationship between NEP and mean BGN_NDVI. It is also possible to estimate fine-scale variation in epipelon densities using hyperspectral imaging (Chennu et al. 2013; Murphy et al. 2004, 2005), although this requires more sophisticated equipment and image processing.

Measuring pelagic concentrations of Chl *a* or other pigments has been criticized for giving an incomplete picture of epipelon communities, and NIR imagery is subject to many of the same criticisms. For example, cell biovolume is a better measure of the materials and nutrients that are incorporated into microalgae, and cell biovolume and species composition are better measures of the potential rate at which microalgae communities can uptake nutrients (Canfield et al. 2019; Felip and Catalan 2000; Geider 1987; Jakobsen and Markager 2016; Wetzel 2001). Even though Chl *a* may be more directly tied to the rate of photosynthesis than other measures of microalgae abundance, it only measures the potential for photosynthesis; realized photosynthetic rates also depend on light, nutrients, temperature, and suitable environmental conditions (Geider 1987). Furthermore, Chl *a* may be poorly related to biovolume due to the physiological response of microalgae to light conditions. In our third lab experiment (Fig. 4), BGN_NDVI was higher under low light than under high light. While this might have been caused by phototoxicity, the high light levels were within the range normally experienced by the Mývatn benthos. Studies have shown that diatoms and other algae increase investment in chloroplasts under low light conditions (Canfield et al. 2019; Felip and Catalan 2000; Geider 1987), and we have seen this response in other experiments and field observations in winter. Although NIR imagery is subject to many of the criticisms of fluorometry on extracted sediment samples as a measure of microalgal abundance, NIR imagery is less subject to the criticism that fluorometry on extracted samples cannot account for self-shading of Chl *a* within or among algal cells; because NIR imagery measures reflectance, it is proportional to exposure from a directional light source such as the sun.

As a laboratory tool, NIR imagery has the advantage of being nondestructive, fast, and cheap, allowing measurement of hundreds of samples daily. Repeated sampling makes it possible to observe changes that evolve in samples (e.g., Fig. 4). There are potential methods that might give more accurate measurements of Chl *a* and other pigments. For example, hyperspectral imagery has the potential to separate different algal groups using differences in reflectance spectra. Nonetheless, this requires calibration against samples of known species composition. In vivo fluorometry uses the specific optical properties of Chl *a* and other pigments to give separate estimates of the densities of taxonomic groups (e.g., diatoms, cyanobacteria, and chlorophytes), yet in vivo fluorometry requires specialized equipment rather than a simple camera. Also, the ability of NIR imagery to transfer between lab and field makes it possible to relate lab and field results.

Comments and recommendations

In our application of NIR imagery, we did not use a white or gray reference card to measure reflectance of the light source (Kromkamp et al. 2006; Murphy et al. 2005). In the lab, we could not use a reference card for photos of submerged samples without disturbing the sediment, and in the field fouling by biofilms will quickly degrade the reference card. Nonetheless, for a standardized light source in the lab, BGN_NDVI gives the relative values which for many applications, such as measuring response to experimental treatments, is sufficient. For field applications, standardizing among images relies on the reflectance in the blue and green spectral bands, and while this seems adequate for images taken relatively close in time, it is problematic to compare images taken, for example, under different water clarity conditions due to shading from phytoplankton and suspended particulates. Thus, in long-term deployments, NIR imagery will be most useful for measuring short-term changes such as wind-induced sediment mixing (Fig. 7).

Despite the potential value of NIR imagery, it has not been used extensively to measure epipelon in the literature. Lack of broad adoption might be because past assessments of the association between simple spectral indices like NDVI and Chl *a* measured by chemically extracting Chl *a* from sediment samples have not been convincing; a comprehensive assessment of the association between the two methods had R^2 values of at most 0.5 (Murphy et al. 2005). However, our results with NIR imagery did not leave us wondering whether NIR imagery could match the performance of measuring Chl *a* from extracted samples, but instead convinced us that NIR imagery was the better method for many applications.

Near-infrared imaging has the potential to aid studies designed to quantify epipelon densities at both fine and broad spatial scales in a lake, giving insight into the contribution that the benthos makes to lake production. At fine spatial scales, infaunal and epifaunal species may play roles as ecosystem engineers that alter primary production through bioturbation and sediment surface alteration (Holdren and Armstrong 1980; Holker et al. 2015; Michael et al. 2023; Phillips et al. 2021; Vaughn and Hakenkamp 2001). The fine-scale variation in Chl *a* generated by ecosystem engineers can be quantified using NIR images (Fig. 1b,c), and the nondestructive imaging makes it possible to observe changes in the benthos through time. Linking Chl *a* measurements to fine-scale patterns of NEP should make it possible to estimate, through space and time, how ecosystem engineers increase or decrease benthic NEP. At the broad whole-lake scale, the ease of taking and processing NIR images makes it possible to characterize the variation in Chl *a* concentration in

the epipelon throughout a lake. Characterizing broad-scale patterns may reveal the effects of light/depth gradients (Gushulak et al. 2021) or proximity to nutrient inflows for benthic NEP (Blumenshine et al. 1997; Hagerthey and Kerfoot 2005). This spatial and temporal variation in epipelon could influence the release of nutrients from the sediment into the pelagic zone (Chen et al. 2018; Dodds 2003). As a caution, patterns in epipelon Chl *a* need to be tested for their ability to predict NEP, because intracellular concentration of Chl *a* may change under different light levels (e.g., Fig. 4) and nutrient availability may limit production. Nonetheless, documenting whole-lake spatial and temporal variation in benthic Chl *a* is an important component of quantifying the contribution of the benthos to whole-lake NEP (Vander Zanden and Vadeboncoeur 2020). Fine- and broad-scale measurements of benthic Chl *a* and NEP will complement the corresponding fine- and broad-scale measurements of pelagic Chl *a* that are possible with recent technological advances (Loken et al. 2018).

We started to investigate NIR imaging because we needed a simple method to measure a proxy for microalgae density on the surface of soft sediments; the diatomaceous ooze of Mývatn becomes resuspended with slight disturbances to the overlying water. We also wanted a method that could be used in the lab and extended field deployments, and by students using cheap and robust equipment. Near-infrared imaging gives a surprisingly accurate way to estimate epipelon densities that is closely related to NEP under lab conditions with saturating light (Fig. 5).

Acknowledgments

This work was funded by US National Science Foundation Long-Term Research in Environmental Biology (LTREB) program (Grants DEB-1052160 and DEB-2134446).

References

Androuin, T., L. Polerecky, P. Decottignies, et al. 2018. "Subtidal Microphytobenthos: A Secret Garden Stimulated by the Engineer Species *Crepidula fornicata*." *Frontiers in Marine Science* 5. https://doi.org/10.3389/fmars.2018.00475.

Anon. 1991. "Committee of Experts for Lake Myvatn Research: Effects of the operations of Kisilidjan Inc. on the Lake Myvatn biota." Iceland Ministry of the Environment [Report]. Iceland: Icelandic Government.

Arar, E. J., and G. B. Collins. 1997. "Vitro Determination of Chlorophyll a and Pheophytin a in Marine and Freshwater Algae by Fluorescence." National Exposure Research Laboratory Report 445.0-1. Washington D.C.: U. S. Environmental Protection Agency. https://cfpub.epa.gov/si/si_public_record_report.cfm?Lab=NERL&dirEntryId=309417.

Barillé, L., A. Le Bris, V. Méléder, et al. 2017. "Photosynthetic Epibionts and Endobionts of Pacific Oyster Shells From Oyster Reefs in Rocky vs. Mudflat Shores." *PLoS One* 12. https://doi.org/10.1371/journal.pone.0185187.

Bertone, E., M. A. Burford, and D. P. Hamilton. 2018. "Fluorescence Probes for Real-Time Remote Cyanobacteria Monitoring: A Review of Challenges and Opportunities." *Water Research* 141: 152–162. https://doi.org/10.1016/j.watres.2018.05.001.

Blumenshine, S. C., Y. Vadeboncoeur, D. M. Lodge, K. L. Cottingham, and S. E. Knight. 1997. "Benthic-Pelagic Links: Responses of Benthos to Water-Column Nutrient Enrichment." *Journal of the North American Benthological Society* 16: 466–479. https://doi.org/10.2307/1468138.

Botsch, J. C., K. R. Book, J. S. Phillips, and A. R. Ives. 2023. "Aquatic Insects Balance Growth With Future Supply of Algal Food Resources." *Oikos* 2023: e09902. https://doi.org/10.1111/oik.09902.

Canfield, D. E., Jr., R. W. Bachmann, M. V. Hoyer, L. S. Johansson, M. Søndergaard, and E. Jeppesen. 2019. "To Measure Chlorophyll or Phytoplankton Biovolume: An Aquatic Conundrum With Implications for the Management of Lakes." *Lake and Reservoir Management* 35: 181–192. https://doi.org/10.1080/10402381.2019.1607958.

Cartaxana, P., M. Ruivo, C. Hubas, I. Davidson, J. Serôdio, and B. Jesus. 2011. "Physiological vs. Behavioral Photoprotection in Intertidal Epipelic and Epipsammic Benthic Diatom Communities." *Journal of Experimental Marine Biology and Ecology* 405: 120–127. https://doi.org/10.1016/j.jembe.2011.05.027.

Chapman, M. G., T. J. Tolhurst, R. J. Murphy, and A. J. Underwood. 2010. "Complex and Inconsistent Patterns of Variation in Benthos, Micro-Algae and Sediment over Multiple Spatial Scales." *Marine Ecology Progress Series* 398: 33–47. https://doi.org/10.3354/meps08328.

Chen, M. S., S. Ding, X. Chen, et al. 2018. "Mechanisms Driving Phosphorus Release during Algal Blooms Based on Hourly Changes in Iron and Phosphorus Concentrations in Sediments." *Water Research* 133: 153–164. https://doi.org/10.1016/j.watres.2018.01.040.

Chennu, A., P. Färber, N. Volkenborn, et al. 2013. "Hyperspectral Imaging of the Microscale Distribution and Dynamics of Microphytobenthos in Intertidal Sediments." *Limnology and Oceanography: Methods* 11: 511–528. https://doi.org/10.4319/lom.2013.11.511.

Chennu, A., A. Grinham, L. Polerecky, D. de Beer, and M. A. A. Al-Najjar. 2015. "Rapid Reactivation of Cyanobacterial Photosynthesis and Migration upon Rehydration of Desiccated Marine Microbial Mats." *Frontiers in Microbiology* 6. https://doi.org/10.3389/fmicb.2015.01472.

Daggers, T. D., J. C. Kromkamp, P. M. J. Herman, and D. van der Wal. 2018. "A Model to Assess Microphytobenthic Primary Production in Tidal Systems Using Satellite Remote Sensing." *Remote Sensing of Environment* 211: 129–145. https://doi.org/10.1016/j.rse.2018.03.037.

Dodds, W. K. 2003. "The Role of Periphyton in Phosphorus Retention in Shallow Freshwater Aquatic Systems." *Journal of Phycology* 39: 840–849. https://doi.org/10.1046/j.1529-8817.2003.02081.x.

Dumke, I., S. M. Nornes, A. Purser, et al. 2018a. "First Hyperspectral Imaging Survey of the Deep Seafloor: High-Resolution Mapping of Manganese Nodules." *Remote Sensing of Environment* 209: 19–30. https://doi.org/10.1016/j.rse.2018.02.024.

Dumke, I., A. Purser, Y. Marcon, et al. 2018b. "Underwater Hyperspectral Imaging as an *In Situ* Taxonomic Tool for Deep-Sea Megafauna." *Scientific Reports* 8: 12860. https://doi.org/10.1038/s41598-018-31261-4.

Einarsson, A., G. Stefansdottir, H. Jóhannesson, et al. 2004. "The Ecology of Lake Myvatn and the River Laxa: Variation in Space and Time." *Aquatic Ecology* 38: 317–348. https://doi.org/10.1023/B:AECO.0000032090.72702.a9.

Felip, M., and J. Catalan. 2000. "The Relationship Between Phytoplankton Biovolume and Chlorophyll in a Deep Oligotrophic Lake: Decoupling in their Spatial and Temporal Maxima." *Journal of Plankton Research* 22: 91–106. https://doi.org/10.1093/plankt/22.1.91.

Geider, R. J. 1987. "Light and Temperature Dependence of the Carbon to Chlorophyll *a* Ratio in Microalgae and Cyanobacteria: Implications for Physiology and Growth of Phytoplankton." *New Phytologist* 106: 1–34. http://www.jstor.org/stable/2434683.

Ghunowa, K., A. S. Medeiros, and R. Bello. 2019. "Hyperspectral Analysis of Algal Biomass in Northern Lakes, Churchill, MB, Canada." *Arctic Science* 5: 240–256. https://doi.org/10.1139/as-2018-0030.

Gomoiu, M.-T. 1967. "Some Quantitative Data on Light Penetration in Sediments." *Helgoländer Wissenschaftliche Meeresuntersuchungen* 15: 120–127. https://doi.org/10.1007/BF01618614.

Gushulak, C. A. C., H. A. Haig, M. Kingsbury, B. Wissel, B. F. Cumming, and P. R. Leavitt. 2021. "Effects of Spatial Variation in Benthic Phototrophs Along a Depth Gradient on Assessments of Whole-Lake Processes." *Freshwater Biology* 66: 2118–2132. https://doi.org/10.1111/fwb.13820.

Hagerthey, S. E., and W. C. Kerfoot. 2005. "Spatial Variation in Groundwater-Related Resource Supply Influences Freshwater Benthic Algal Assemblage Composition." *Journal of the North American Benthological Society* 24: 807–819. https://doi.org/10.1899/04-004.1.

Holdren, G. C., and D. E. Armstrong. 1980. "Factors Affecting Phosphorus Release From Intact Lake Sediment Cores." *Environmental Science & Technology* 14: 79–87. https://doi.org/10.1021/es60161a014.

Holker, F., M. J. Vanni, J. J. Kuiper, et al. 2015. "Tube-Dwelling Invertebrates: Tiny Ecosystem Engineers Have Large Effects in Lake Ecosystems." *Ecological Monographs* 85: 333–351. https://doi.org/10.1890/014-1160.1.

Holm-Hansen, O., C. J. Lorenzen, R. W. Holmes, and J. D. H. Strickland. 1965. "Fluorometric Determination of Chlorophyll." *ICES Journal of Marine Science* 30: 3–15. https://doi.org/10.1093/icesjms/30.1.3.

Hope, J. A., D. M. Paterson, and S. F. Thrush. 2020. "The Role of Microphytobenthos in Soft-Sediment Ecological Networks and Their Contribution to the Delivery of Multiple Ecosystem Services." *Journal of Ecology* 108: 815–830. https://doi.org/10.1111/1365-2745.13322.

Huot, Y., and M. Babin. 2011. "Overview of Fluorescence Protocols: Theory, Basic Concepts, and Practice." In Chlorophyll-a Fluorescence in Aquatic Sciences: Methods and Applications, edited by D. J. Suggett, M. A. Borowitzka, and O. Prasil, 31–74. Dordrecht: Springer Science+Business Media. https://doi.org/10.1007/978-90-481-9268-7_3.

Ives, A. R. 2021. "LTREB Chemical and Physical Limnology at Lake Myvatn 2012-Current, Deprecated ver 2." Environmental Data Initiative https://edirepository.org.

Jacobs, P., J. Pitarch, J. C. Kromkamp, and C. J. M. Philippart. 2021. "Assessing Biomass and Primary Production of Microphytobenthos in Depositional Coastal Systems Using Spectral Information." *PLoS One* 16: e0246012. https://doi.org/10.1371/journal.pone.0246012.

Jakobsen, H. H., and S. Markager. 2016. "Carbon-to-Chlorophyll Ratio for Phytoplankton in Temperate Coastal Waters: Seasonal Patterns and Relationship to Nutrients." *Limnology and Oceanography* 61: 1853–1868. https://doi.org/10.1002/lno.10338.

Jesus, B., P. Rosa, J. L. Mouget, V. Méléder, P. Launeau, and L. Barillé. 2014. "Spectral-Radiometric Analysis of Taxonomically Mixed Microphytobenthic Biofilms." *Remote Sensing of Environment* 140: 196–205. https://doi.org/10.1016/j.rse.2013.08.040.

Kazemipour, F., V. Méléder, and P. Launeau. 2011. "Optical Properties of Microphytobenthic Biofilms (MPBOM): Biomass Retrieval Implication." *Journal of Quantitative Spectroscopy and Radiative Transfer* 112: 131–142. https://doi.org/10.1016/j.jqsrt.2010.08.029.

Koh, C. H., J. S. Khim, H. Araki, H. Yamanishi, and K. Koga. 2007. "Within-Day and Seasonal Patterns of Microphytobenthos Biomass Determined by co-Measurement of Sediment and Water Column Chlorophylls in the Intertidal Mudflat of Nanaura, Saga, Ariake Sea, Japan." *Estuarine, Coastal and Shelf Science* 72: 42–52. https://doi.org/10.1016/j.ecss.2006.10.005.

Kromkamp, J. C., E. Morris, and R. M. Forster. 2020. "Microscale Variability in Biomass and Photosynthetic Activity of Microphytobenthos during a Spring-Neap Tidal Cycle." *Frontiers in Marine Science* 7. https://doi.org/10.3389/fmars.2020.00562.

Kromkamp, J. C., E. P. Morris, R. M. Forster, C. Honeywill, S. Hagerthey, and D. M. Paterson. 2006. "Relationship of Intertidal Surface Sediment Chlorophyll Concentration to

Hyperspectral Reflectance and Chlorophyll Fluorescence." *Estuaries and Coasts* 29: 183–196. https://doi.org/10.1007/bf02781988.

Kühl, M., C. Lassen, and B. B. Jorgensen. 1994. "Light Penetration and Light Intensity in Sandy Marine Sediments Measured With Irradiance and Scalar Irradiance Fiber-Optic Microprobes." *Marine Ecology-Progress Series* 105: 139–148. https://doi.org/10.3354/meps105139.

Kutser, T., J. Hedley, C. Giardino, C. Roelfsema, and V. E. Brando. 2020. "Remote Sensing of Shallow Waters – A 50 Year Retrospective and Future Directions." *Remote Sensing of Environment* 240: 111619. https://doi.org/10.1016/j.rse.2019.111619.

Loken, L. C., J. T. Crawford, M. M. Dornblaser, et al. 2018. "Limited Nitrate Retention Capacity in the Upper Mississippi River." *Environmental Research Letters* 13: 074030. https://doi.org/10.1088/1748-9326/aacd51.

Maggi, E., A. C. Jackson, T. Tolhurst, A. J. Underwood, and M. G. Chapman. 2013. "Changes in Microphytobenthos Fluorescence over a Tidal Cycle: Implications for Sampling Designs." *Hydrobiologia* 701: 301–312. https://doi.org/10.1007/s10750-012-1291-x.

McCormick, A. R., J. S. Phillips, J. C. Botsch, and A. R. Ives. 2021. "Shifts in the Partitioning of Benthic and Pelagic Primary Production Within and across Summers in Lake Mývatn, Iceland." *Inland Waters* 11: 13–28. https://doi.org/10.1080/20442041.2020.1859868.

McCormick, A. R., J. S. Phillips, and A. R. Ives. 2019. "Responses of Benthic Algae to Nutrient Enrichment in a Shallow Lake: Linking Community Production, Biomass, and Composition." *Freshwater Biology* 64: 1833–1847. https://doi.org/10.1111/fwb.13375.

Michael, T. C., D. M. Costello, A. S. Fitzgibbon, and L. E. Kinsman-Costello. 2023. "Invertebrate Activities in Wetland Sediments Influence Oxygen and Nutrient Dynamics at the Sediment–Water Interface." *Wetlands* 43: 9. https://doi.org/10.1007/s13157-023-01737-9.

Mogstad, A. A., G. Johnsen, and M. Ludvigsen. 2019. "Shallow-Water Habitat Mapping Using Underwater Hyperspectral Imaging From an Unmanned Surface Vehicle: A Pilot Study." *Remote Sensing* 11: 685. https://doi.org/10.3390/rs11060685.

Montes-Herrera, J. C., E. Cimoli, V. Cummings, N. Hill, A. Lucieer, and V. Lucieer. 2021. "Underwater Hyperspectral Imaging (UHI): A Review of Systems and Applications for Proximal Seafloor Ecosystem Studies." *Remote Sensing* 13: 3451. https://doi.org/10.3390/rs13173451.

Murphy, R. J., T. J. Tolhurst, M. G. Chapman, and A. J. Underwood. 2004. "Estimation of Surface Chlorophyll on an Exposed Mudflat Using Digital Colour-Infrared (CIR) Photography." *Estuarine, Coastal and Shelf Science* 59: 625–638. https://doi.org/10.1016/j.ecss.2003.11.006.

Murphy, R. J., T. J. Tolhurst, M. G. Chapman, and A. J. Underwood. 2005. "Estimation of Surface Chlorophyll-a on an Emersed Mudflat Using Field Spectrometry: Accuracy of Ratios and Derivative-Based Approaches." *International Journal of Remote Sensing* 26: 1835–1859. https://doi.org/10.1080/01431160512331326530.

Murphy, R. J., and A. J. Underwood. 2006. "Novel Use of Digital Colour-Infrared Imagery to Test Hypotheses About Grazing by Intertidal Herbivorous Gastropods." *Journal of Experimental Marine Biology and Ecology* 330: 437–447. https://doi.org/10.1016/j.jembe.2005.09.006.

Murphy, R. J., A. J. Underwood, and A. C. Jackson. 2009. "Field-Based Remote Sensing of Intertidal Epilithic Chlorophyll: Techniques Using Specialized and Conventional Digital Cameras." *Journal of Experimental Marine Biology and Ecology* 380: 68–76. https://doi.org/10.1016/j.jembe.2009.09.002.

O'Reilly, J. E., and P. J. Werdell. 2019. "Chlorophyll Algorithms for Ocean Color Sensors – OC4, OC5 & OC6." *Remote Sensing of Environment* 229: 32–47. https://doi.org/10.1016/j.rse.2019.04.021.

Phillips, J. S., A. R. McCormick, J. C. Botsch, and A. R. Ives. 2021. "Ecosystem Engineering Alters Density-Dependent Feedbacks in an Aquatic Insect Population." *Ecology* 102: e03513. https://doi.org/10.1002/ecy.3513.

R Core Team. 2023. R: A Language and Environment for Statistical Computing. 4.1.0 ed. Austria: R Foundation for Statistical Computing.

Russell, B. J., H. M. Dierssen, L. J. TC, et al. 2016. "Spectral Reflectance of Palauan Reef-Building Coral With Different Symbionts in Response to Elevated Temperature." *Remote Sensing* 8: 164. https://doi.org/10.3390/rs8030164.

Stock, W., L. Blommaert, I. Daveloose, W. Vyverman, and K. Sabbe. 2019. "Assessing the Suitability of Imaging-PAM Fluorometry for Monitoring Growth of Benthic Diatoms." *Journal of Experimental Marine Biology and Ecology* 513: 35–41. https://doi.org/10.1016/j.jembe.2019.02.003.

Summers, N., G. Johnsen, A. Mogstad, H. Lovås, G. Fragoso, and J. Berge. 2022. "Underwater Hyperspectral Imaging of Arctic Macroalgal Habitats During the Polar Night Using a Novel Mini-ROV-UHI Portable System." *Remote Sensing* 14: 1325. https://doi.org/10.3390/rs14061325.

Tong, Y., L. Feng, D. Zhao, W. Xu, and C. Zheng. 2022. "Remote Sensing of Chlorophyll-a Concentrations in Coastal Oceans of the Greater Bay Area in China: Algorithm Development and Long-Term Changes." *International Journal of Applied Earth Observation and Geoinformation* 112: 102922. https://doi.org/10.1016/j.jag.2022.102922.

Tucker, C. J. 1979. "Red and Photographic Infrared Linear Combinations for Monitoring Vegetation." *Remote Sensing of Environment* 8: 127–150. https://doi.org/10.1016/0034-4257(79)90013-0.

Urbanek, S. 2022. "Jpeg: Read and Write JPEG Images." https://cran.r-project.org/web/packages/jpeg/jpeg.pdf.

Vander Zanden, M. J., and Y. Vadeboncoeur. 2020. "Putting the Lake Back Together 20 Years Later: What in the Benthos Have We Learned About Habitat Linkages in Lakes?" *Inland Waters* 10: 305–321. https://doi.org/10.1080/20442041.2020.1712953.

Vaughn, C. C., and C. C. Hakenkamp. 2001. "The Functional Role of Burrowing Bivalves in Freshwater Ecosystems." *Freshwater Biology* 46: 1431–1446. https://doi.org/10.1046/j.1365-2427.2001.00771.x.

Wetzel, R. G. 2001. Limnology: Lake and River Ecosystems. 3rd ed. San Francisco: Academic Press.

Zhang, T., B. Tian, Y. Wang, et al. 2021. "Quantifying Seasonal Variations in Microphytobenthos Biomass on Estuarine Tidal Flats Using Sentinel-1/2 Data." *Science of the Total Environment* 777: 146051. https://doi.org/10.1016/j.scitotenv.2021.146051.

Supporting Information

Additional Supporting Information may be found in the online version of this article.

Submitted 20 August 2024
Revised 23 December 2024
Accepted 20 January 2025